NUCLEAR STRUCTURE -- EXPERIMENT

THE (^{6}Li,^{6}He) REACTION AS A PROBE OF SPIN STRENGTH: STUDIES AT 14, 25 AND 35 MEV/NUCLEON.

J.S. Winfield, N. Anantaraman, S.M. Austin, C.C. Chang,[a] Z. Chen, G. Ciangaru,[b] A. Galonsky, J. van der Plicht, and H.-L. Wu

Following our study[1] of GT transitions induced by the (^{6}Li,^{6}He) reaction at a bombarding energy of 35 MeV/nucleon, we have taken similar data for ^{6}Li energies of 25 and 14 MeV/nucleon. The targets studied were ^{7}Li, ^{12,14}C and, at 25 MeV/nucleon only, ^{90}Zr. The main objective of this survey of the (^{6}Li,^{6}He) reaction is to investigate the importance of the one-step reaction mechanism relative to the competing higher-order processes. If the one-step mechanism dominates, the spins and parities of ^{6}Li and ^{6}He impose a spin transfer of $\Delta S=1$, so that at forward angles where $\Delta L=0$ transfers are strong, the reaction should be a good probe of Gamow-Teller (GT) strength. At more backward angles, higher multipolarity spin-flip excitations may be observed.

Measurements were performed with the S-320 spectrograph and its focal plane detector. A spectrum for ^{14}C(^{6}Li,^{6}He)^{14}N at 14 MeV/nucleon is displayed in Fig. 1. Typically, a resolution of $\Delta E/E \approx 1/600$ was obtained. For the lower bombarding energies, the absolute resolution is thus significantly better than in state-of-the-art intermediate-energy (p,n) experiments.

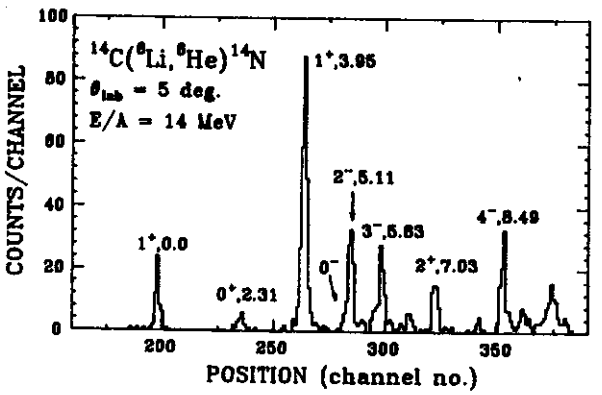

Fig. 1 Spectrum of ^{14}C(^{6}Li,^{6}He)^{14}N for E(^{6}Li) = 14 MeV/nucleon and a spectrograph angle of 5°. States in ^{14}N are indicated with the excitation energy given in MeV. The observed resolution is 140 keV.

A simple model-independent test of the nature of the reaction mechanism is to compare the ratio of one-step allowed and one-step suppressed transitions to states in the residual nuclei. In Table I we compare the relative cross sections of the 0.0, 2.31 and 3.95 MeV states of ^{14}N. The 1$^+$ ground state has a B(GT) value from β-decay only about 10^{-5} of that for the 3.95 MeV level, and in the (p,n) reaction the ratio of cross sections is observed to be 0.01. For (^{6}Li,^{6}He), the ratio varies from 0.1 at 35 MeV/nucleon to 0.2 at 14 MeV/nucleon, and appears to continue to increase at lower bombarding energies. However, tensor and exchange terms in the interaction or $\Delta L=2$ transfer may account for the differences between the various reactions and the dependence of the ratios for (^{6}Li,^{6}He) on energy. A better test of the contribution of two-step processes is the ratio of the 0$^+$ isobaric analog state (IAS) at 2.31 MeV to the 3.95 MeV state, because a 0$^+$ to

Table I. Ratios of yields to three states in ^{14}N observed with the ^{14}C(^{6}Li,^{6}He) reaction for different ^{6}Li bombarding energies. In each case the comparisons are done at $q \approx 0.5$ fm^{-1}.

E/A (MeV)	$\frac{\sigma(1^+,0.0)}{\sigma(1^+,3.95)}$	$\frac{\sigma(0^+,2.31)}{\sigma(1^+,3.95)}$
35	0.11	0.05
25	0.15	0.05
14	0.21	0.08
10	0.30[a]	0.1[a]

a) estimated from Ref. 2.

0^+ transition can only be mediated by the non-local part of the exchange interaction in a one-step process. Table I shows that at 35 and 25 MeV/nucleon the IAS is suppressed by a factor of two compared with results[2] at 10 MeV/nucleon, which indicates that multi-step processes are giving a stronger contribution at the lower energies.

In Table II, the ratio of cross sections for the ground and 0.43 MeV excited states of ^{7}Be are listed for comparison with the ratio of B(GT) values known from β-decay. The first column, which is the ratio averaged over all angles, is larger at all energies than the ratio of B(GT) values, 1.18. However, in the last column of this table (which gives the ratio for the smallest angles studied in each case), at 35 MeV/nucleon the (^{6}Li,^{6}He) ratio is in agreement with the B(GT) ratio; there is a trend away from this value as the bombarding energy is reduced. The inconsistent results for the larger angles studied may be due to sizeable contributions from the tensor interaction at different momentum transfers (compare the angle-dependance of the tensor interaction in the ^{7}Li(p,n)^{7}Be reaction as shown in Ref. 3).

Table II. Ratios of yields to the ground and first excited states in ^{7}Be observed with the ^{7}Li(^{6}Li,^{6}He) reaction for different ^{6}Li bombarding energies. The second column gives the unweighted mean of the ratios for all angles studied (typically from 2.5° to 5.5° lab.), the third column gives the ratio at the smallest angle only.

E/A (MeV)	$\sigma(3/2^-,0.0)/\sigma(1/2^-,0.43)$ all θ's	θ ≈ 2.5°
35	1.46±0.10	1.08±0.06
25	1.47±0.08	1.34±0.07
14	1.66±0.06	1.78±0.05

A second class of tests of the reaction mechanism is to compare the data with one-step distorted wave Born approximation (DWBA) calculations. In Fig. 2, angular distributions are shown for the calculations completed so far; others are in progress. The DWBA code used is a modified version[4] of DWUCK which allows for the finite size of the projectile system and includes direct ($V_{\sigma\tau}$) + exchange + tensor terms in the interaction. Optical potentials obtained[5] from 150 MeV ^{6}Li elastic scattering

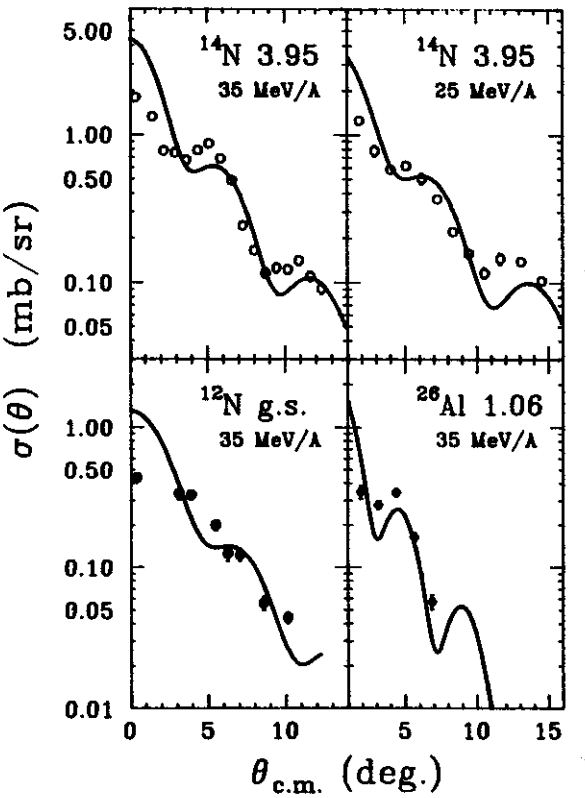

Fig. 2 Angular distributions for the (^{6}Li,^{6}He) reaction on targets of ^{14}C, ^{12}C and ^{26}Mg. The final state nucleus and excitation energy is indicated in each case. Curves are DWBA calculations normalized to the data.

data were used. For the mass-14 and mass-12 systems, shell-model wave functions from an interaction due to Millener[6] were used; for the mass-26 system, the Wildenthal[7] interaction was used. The normalizations of the curves required to fit the data, with a Yukawa interaction of 1

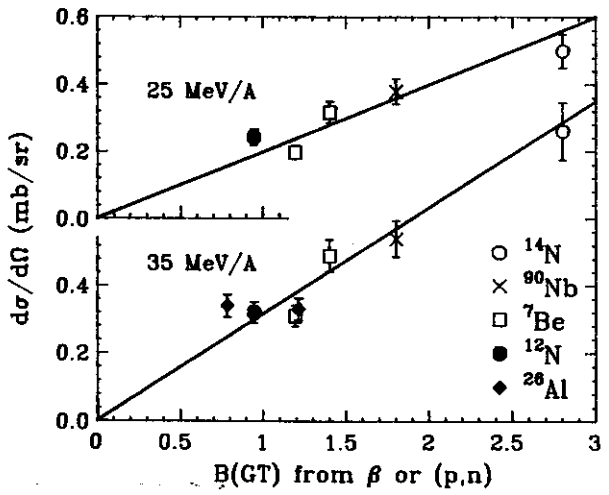

Fig. 3 Plot of cross sections at $qR/R(^{14}C) = 100$ MeV/c for various GT transitions induced by (^{6}Li,^{6}He) at 25 and 35 MeV/nucleon. The final states, with excitation energies in MeV, are: ^{14}N(3.95), ^{90}Nb(2.3), ^{12}N(0.0), ^{7}Be(0.0 and 0.43), and ^{26}Al(1.06 and 1.85).

fm range and with the Millener wave functions renormalized to give the experimental B(GT) value, correspond to $V_{\sigma\tau}$ values ranging from 7 to 14 MeV. This is to be compared with the average value of 11.7±1.7 MeV obtained[8] from (p,n) studies at similar energies/nucleon. However, the calculations overpredict the data at small angles, possibly because of the lack of appropriate optical model potentials or the neglect of the exchange part of the tensor interaction.

We have investigated how closely the observed forward-angle 1^{+} cross sections measure Gamow-Teller strength. Goodman et al.[8] have shown that high energy (p,n) 0° cross sections are well correlated with the corresponding β-decay matrix elements. Figure 3 shows the cross sections for various GT transitions at qR/R_{14C} = 100 MeV/c, where q is the linear momentum transfer and R/R_{14C} is defined as $1.3(A_T^{1/3}+A_P^{1/3})/5.495$ (the denominator scales the radii to that of ^{6}Li+^{14}C). At 14 MeV/nucleon the overlap of equivalent qR values is too limited and we do not show this data, but at 25 and 35 MeV/nucleon there does appear to be a high degree of proportionality.

In summary, the ratios of observed cross sections for certain states in ^{14}N and ^{7}Be indicate that the contribution to the (^{6}Li,^{6}He) reaction from higher-order processes is increasingly noticeable as the bombarding energy is reduced. However, the proportionality between the cross sections for GT transitions and β-decay matrix elements which was observed[1] at 35 MeV/nucleon, is maintained at least at 25 MeV/nucleon, and the reaction may still be a useful probe of spin strength in nuclei at even lower energies.

References

a. University of Maryland, College Park, MD.
b. Schlumberger Well Services, Houston, TX.

1. NSCL 1983-84 annual report, p. 102, and to be submitted to Phys. Lett.
2. C.D. Goodman et al., Phys. Lett. 64B,417 (1976); W.R. Wharton et al., Phys. Rev. C 22,1138(1980).
3. S.M. Austin et al., Phys. Rev. Lett. 44,972 (1980).
4. G. Ciangaru et al., Nucl. Phys. A380,147 (1982).
5. J. Cook, Nucl.Phys. A388,153(1982).
6. D.J. Millener, private communication.
7. B.H. Wildenthal, private communication.
8. C.D. Goodman et al., Phys. Rev. Lett. 44, 1755(1980).

AT WHAT ENERGY ARE ONE-STEP PROCESSES DOMINANT IN (^{12}C,^{12}N) REACTIONS?

J.S. Winfield, N. Anantaraman, S.M. Austin, L.H. Harwood, J. van der Plicht, H.-L. Wu, and A.F. Zeller.

Provided that the reaction mechanism is one-step, the spins and parities of the projectile and ejectile make the (^{12}C,^{12}N) reaction selective of $\Delta S=1$ transitions. This, together with the absence of bound excited states in ^{12}N, leads to a potentially very useful probe of Gamow-Teller and other spin-dependent β^+ strength in nuclei. However, if higher-order processes such as the sequential transfer of nucleons contribute significantly to the reaction, the $\Delta S=1$ selectivity may be lost.

As described in last year's annual report, we have studied the ^{12}C(^{12}C,^{12}N)^{12}B reaction at 35 MeV/nucleon and found that one-step DWBA calculations underestimate the data by almost an order of magnitude.[1] We concluded that sequential transfer processes are still dominant at 35 MeV/nucleon, although the relative contribution of the one-step process appears to be greater than that in ^{26}Mg(^{12}C,^{12}B)^{26}Al at 9 MeV/nucleon.[2] For comparison, a preliminary report[3] suggests that the (^{18}O,^{18}F) reaction at 20 MeV/nucleon may be closer to the single-step DWBA prediction. This reaction has a more favorable matrix element than (^{12}C,^{12}N) -- the log(ft) values for β-decay transitions connecting the ground states are 3.55 (^{18}F-^{18}O) and 4.12 (^{12}N-^{12}N) -- but the presence of low-lying bound states in ^{18}F makes the (^{18}O,^{18}F) reaction much less useful for spectroscopy.

There are strong indications[4] that the cross section for sequential transfer will fall rapidly with increasing beam energy. Kurihara and Sakai[5] have noted that with increasing beam energy there is an exponential decrease in the yield of the single-neutron transfer, (p,d) and (^{3}He,α), and of the two-neutron transfer, (p,t) and (α,^{6}He), reactions. Furthermore, the slope parameters for the two-neutron transfer cross sections are approximately double those for the single-neutron transfer. This adds some support to a simple approximation for the sequential transfer cross section given in Ref. 1:

$$\sigma_{seq} \approx \frac{A\,\sigma_1\,\sigma_2}{\sqrt{E}} \approx \frac{A'\,(\sigma_1)^2}{\sqrt{E}} \qquad (1)$$

where σ_1 and σ_2 are the cross sections for single nucleon transfer and A is a constant. The inverse square root dependence on energy is put in as an approximation for the Green's function that mediates the propagation in the intermediate channel; this follows from a formula suggested by Madsen and Brown[6] for two-step (p,n) charge-exchange involving inelastic scattering.

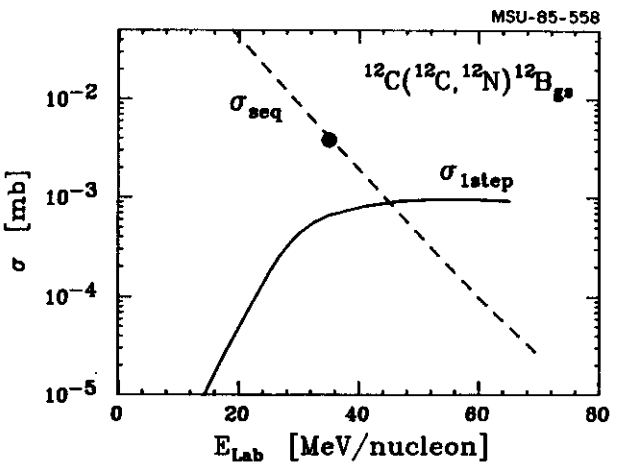

Fig. 1 Energy dependance of σ(seq) and σ(1step) estimated from DWBA calculations. The normalization of σ(seq) was determined from the observed cross section for ^{12}C(^{12}C,^{12}N)^{12}B (g.s.) at 35 MeV/nucleon (represented by the point), with the assumption that this is dominated by sequential transfer processes.

We have calculated the single-nucleon transfer cross section ^{13}C(^{12}C,^{13}C)^{12}C for a range of energies and deduced σ_{seq} from Eq. 1. One-step (^{12}C,^{12}N) cross sections have also been calculated for a range of energies (with a $V_{\sigma\tau}$

interaction strength of 12 MeV), and the energy dependence of the angle-integrated cross sections is shown in Fig. 1. From this figure, we estimate that the sequential transfer contribution to (^{12}C,^{12}N) becomes negligible at about 60 MeV/nucleon. This limit may be reduced to 50 MeV/nucleon if exchange effects (not included in the calculations) increase σ_{1step} by 30%. We plan to test this prediction with a 50 MeV/nucleon ^{12}C beam from the ECR-injected K500 cyclotron.

References

1. J.S. Winfield, N. Anantaraman, S.M. Austin, L.H. Harwood, J. van der Plicht, H.-L. Wu, and A.F. Zeller, Phys. Rev. C (April 1986).
2. A. Etchegoyen, D. Sinclair, S. Liu, M.C. Etchegoyen, D.K. Scott, and D.L. Hendrie, Nucl. Phys. A397,343(1983).
3. B.L. Burks, D.J. Horen, M.A.G. Fernandes, R.L. Auble, F.E. Bertrand, J.L. Blankenship, E.E. Gross, D.C. Hensley, R.O. Sayer, and D. Shapira, Bull. Am. Phys. Soc. 30, 1255(1985).
4. W. von Oertzen, Phys. Lett. 151B,95(1985); in Frontiers of Nuclear Dynamics, edited by R.A. Broglia and C.H. Dasso (Plenum, New York, 1985).
5. T. Kurihara and M. Sakai, Phys. Lett. 133B, 157(1983).
6. V.A. Madsen and V.R. Brown, in The (p,n) Reaction and the N-N force, edited by C.D. Goodman et al. (Plenum, New York, 1980).

SPIN-FLIP TRANSITIONS STUDIED USING THE (p,p') REACTION

C. Djalali, G.M. Crawley, A. Galonsky, N. Marty,[a] M. Morlet,[a] A. Willis[a]

The (p,p') reaction at intermediate energies and at forward angles has proved to be a highly selective probe for exciting L=0, spin-flip (M1) transitions. Such transitions have been studied by an MSU-Orsay collaboration using 201 MeV protons from the Orsay synchrocyclotron in more than forty nuclei ranging from ^{16}O to ^{208}Pb. Most of these results have already been published and presented in previous annual reports. In the past year, new data were obtained for ^{24}Mg and ^{32}S; data with better energy resolution were taken on gaseous targets of ^{16}O, ^{18}O, ^{20}Ne and ^{22}Ne. In this report we will discuss three different topics on which substantial progress has been made in the past year.

1. Low-lying 1^+ states in ^{154}Sm, ^{156}Gd, ^{164}Dy and ^{46}Ti[†].

Differences between proton and electron scattering can be used to obtain information on the spin versus orbital nature of particular transitions and therefore on the structure of the states. We have recently applied this method to some low-lying 1^+ transitions observed in heavy deformed nuclei.[1] These states were first observed in electron scattering[2] and were believed to be mainly orbital transitions arising from a collective "twisting" mode of oscillation of protons against neutrons. However, no direct proof could be given from inelastic electron scattering alone since both spin and orbital parts of the electromagnetic interaction may contribute. If the states were mainly orbital they would not be excited in the (p,p') reaction. Indeed, only upper limits on the cross sections for the (p,p') reaction on ^{154}Sm, ^{156}Gd and ^{164}Dy could be obtained. This suggested that the spin contributions to these excitations were small, thus supporting the earlier suggestion of a dominant orbital mode. In addition, Zamick[3] has recently pointed out that low lying 1^+ states with strong M1 transition strength are not restricted to rare earth nuclei. In an $f_{7/2}$ shell model calculation, he predicted a state at $E_x \sim 4$ MeV carrying a transition strength $B(M1)\uparrow = 1.7\ \mu_N^2$. This stimulated us to explore the role of spin and orbital excitation mechanisms in medium heavy nuclei, specifically in ^{46}Ti.

Spectra on ^{46}Ti from both (p,p') and (e,e') are given in Fig. 1. The energy of the state seen in (p,p') at 4.32 MeV agrees very well with the energy of the state excited by (e,e'). The shape of the measured angular distribution of this state matches that predicted for the low lying 1^+ state by the shell model calculations

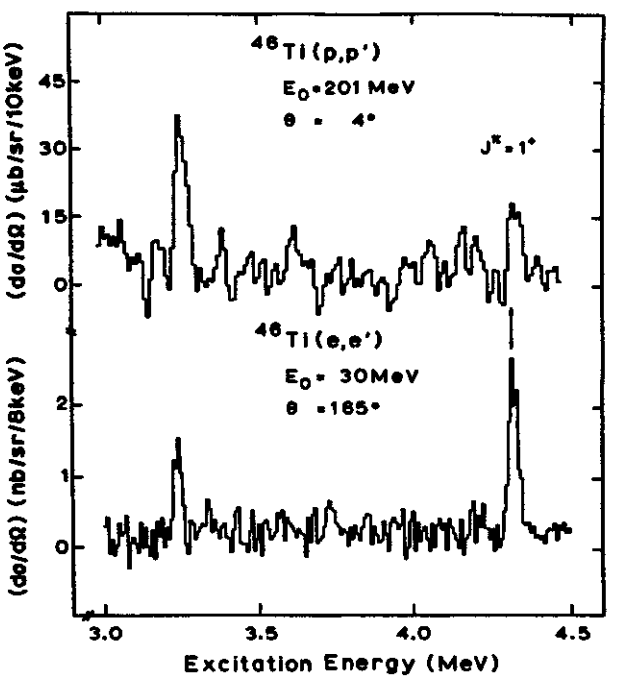

Fig. 1. Comparison between (p,p') and (e,e') background subtracted inelastic scattering spectra on ^{46}Ti .

of Brown. We obtain a B(σ) value of 0.13 ± 0.2 B_N^2, and the B(M1)↑ value from the (e,e') measurement is 1.0 ± 0.2 μ_N^2.

Thus for ^{46}Ti, a measured value of the spin contribution is obtained, in contrast to the situation in the three heavy target nuclei, where we could determine only an upper limit. For all four nuclei, we have shown that the spin contribution to the B(M1)↑ is generally smaller than the orbital contribution, a conclusion that supports the "twist" nature of these states.

2. s-d Shell nuclei

Experimentally, very little is known about isoscalar M1 states since these states are generally not excited in electromagnetic reactions. In intermediate energy (p,p') scattering both isoscalar and isovector M1 states can be excited. The study of these transitions (first carried out in ^{28}Si[4]) has been extended to ^{20}Ne, ^{22}Ne, ^{24}Mg, ^{26}Mg and ^{32}S. A representative spectrum from two of these nuclei is given in Fig. 2. In these light nuclei, the angular distributions are very characteristic of the quantum number (J^π, T) of the states, therefore allowing a clear identification of the quantum numbers. For ^{24}Mg, ^{26}Mg and ^{32}S, we are in the process of making distorted wave calculations for the isoscalar and the isovector 1^+ states, using the wave functions of B.A. Brown and H. Wildenthal.[5]

The ^{20}Ne and ^{22}Ne data were obtained using a gas cell target with Kapton windows. To obtain good energy resolution, the cell had to be fairly thin and was therefore operated at pressures of three to four bars. The resolution becomes worse as the scattering angle increases but we were able to take usable data with this target between laboratory angles of 3° to 10°. The results have been compared to those obtained in gamma ray fluorescence measurements, showing the strong role of the orbital interaction in the electromagnetic excitation of 1^+ states in

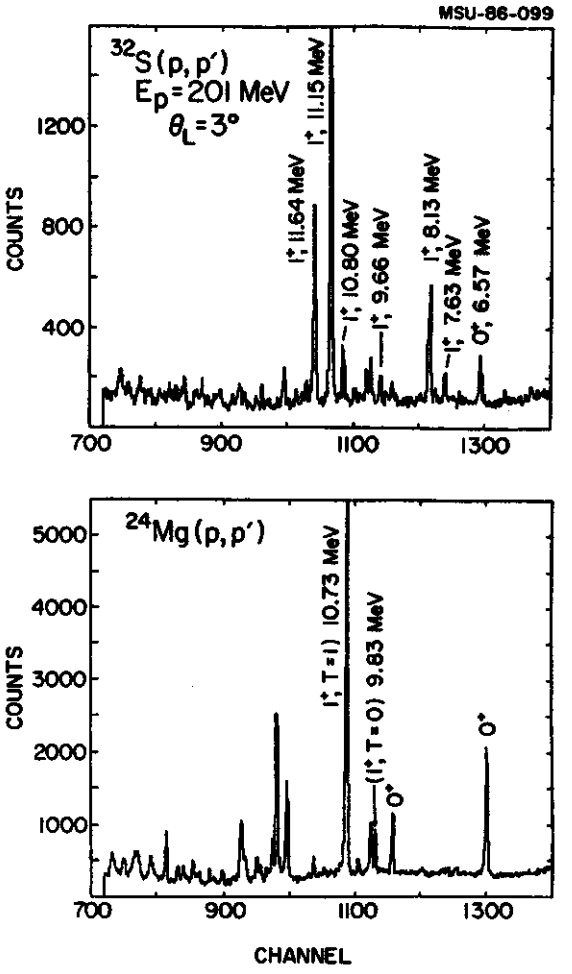

Fig. 2. Spectra of protons inelastically scattered from ^{32}S and ^{24}Mg at 3°.

^{20}Ne and ^{22}Ne. Using Brown and Wildenthal shell model predictions, the ratios of experimental to theoretical strength for M1 transitions in ^{20}Ne and ^{22}Ne are respectively 1.01 and 0.73 .

B. Oxygen isotopes: ^{16}O, ^{18}O

New measurements with improved gas cell targets were taken on ^{16}O and ^{18}O. Spectra measured at 3° are given in Fig 3. In ^{16}O, the three known 1^+ states at 16.22 MeV, 17.14 MeV and 18.77 MeV are clearly excited. Furthermore, a broad structure centered at 14 MeV and having

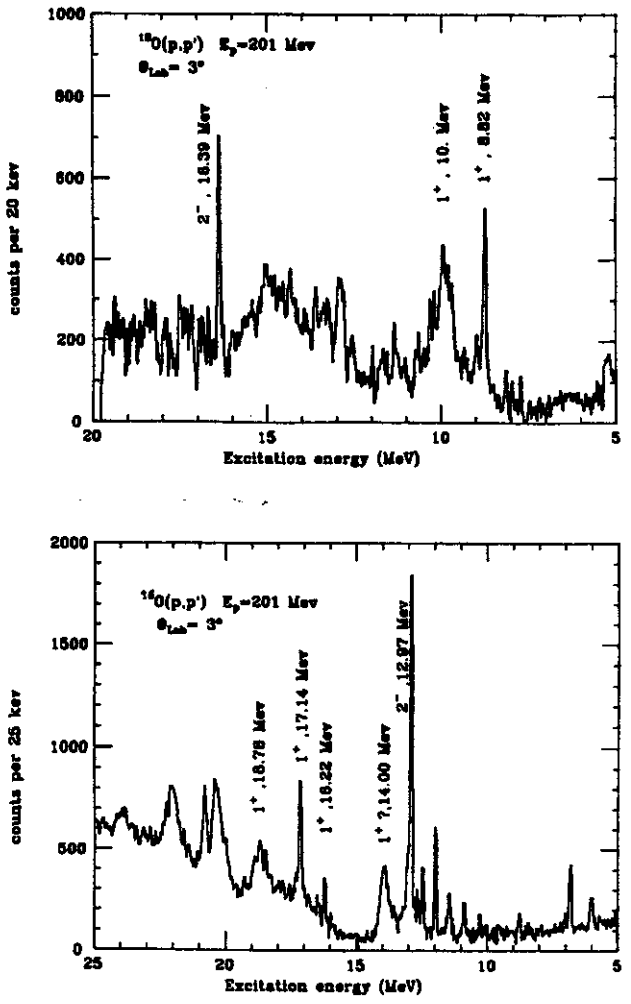

Fig. 3. Spectra of protons inelastically scattered from ^{18}O and ^{16}O at 3°.

a forward peaked angular distribution characteristic of a 1^+ state is observed. In ^{18}O, a level at 8.82 MeV and a broad structure centered at 10 MeV have forward peaked angular distributions and could correspond to M1 transitions. Further work is underway to obtain the absolute cross sections and compare the measured M1 strength to Brown and Wildenthal shell model predictions. A number of M2 transitions are also observed in both nuclei; the comparison with theoretical predictions is underway.

---

a. Institut de Physique Nucleaire, Orsay, France.

† This work was carried out in collaboration with a group from Darmstadt, West Germany.

References

1. C. Djalali, et al., Phys. Lett. 164B (1985) 269
2. D. Bohle et al., Phys. Lett. 137B (1984) 27; Phys Lett 148B (1984) 260
3. L. Zamick, Phys. Rev. C31 (1985) 1955.
4. N. Anantaraman et al., Phys. Rev. Lett. 52 (1984) 1409
5. B.A. Brown and H. Wildenthal, private communication.

ROTATIONAL BANDS IN DEFORMED ODD-ODD NUCLEI

Wen-Tsae Chou, Wade Olivier, Rahmat Aryaeinejad, and Wm. C. McHarris

Until recently in-beam γ-ray spectroscopy of odd-odd nuclei was thought to be unrewardingly cumbersome. During the last several years, however, a number of experimental groups have discovered that, under certain conditions, in-beam γ-ray studies of odd-odd nuclei produce far simpler spectra than expected, with the resulting level schemes yielding a considerable amount of worthwhile information about details of nuclear structure. The necessary conditions appear to be deformed nuclei and/or high-spin states.

In Fig. 1 we show the level scheme produced by the $^{181}Ta(\alpha,3n\gamma)^{182}Re$ reaction.[1] This reaction brings in only a moderate amount of angular momentum; yet most of the deexcitation proceeds through only two high-spin rotational bands, the remainder through two additional low-spin but high-Ω bands. All four bands show considerable distortion -- in particular, a compressed A-term and a non-negligible positive B-term when their energies are fitted to the standard equation,

$$E_J = E_0 + AJ(J+1) + BJ^2(J+1)^2.$$

This type of distortion is characteristic of Coriolis coupling, where the matrix elements have the form,

$$-\hbar^2/2\ [j(j+1) - \Omega(\Omega \pm 1)]^{1/2} \times [J(J+1) - K(K \pm 1)]^{1/2}.$$

Thus, a perturbation expansion results in a

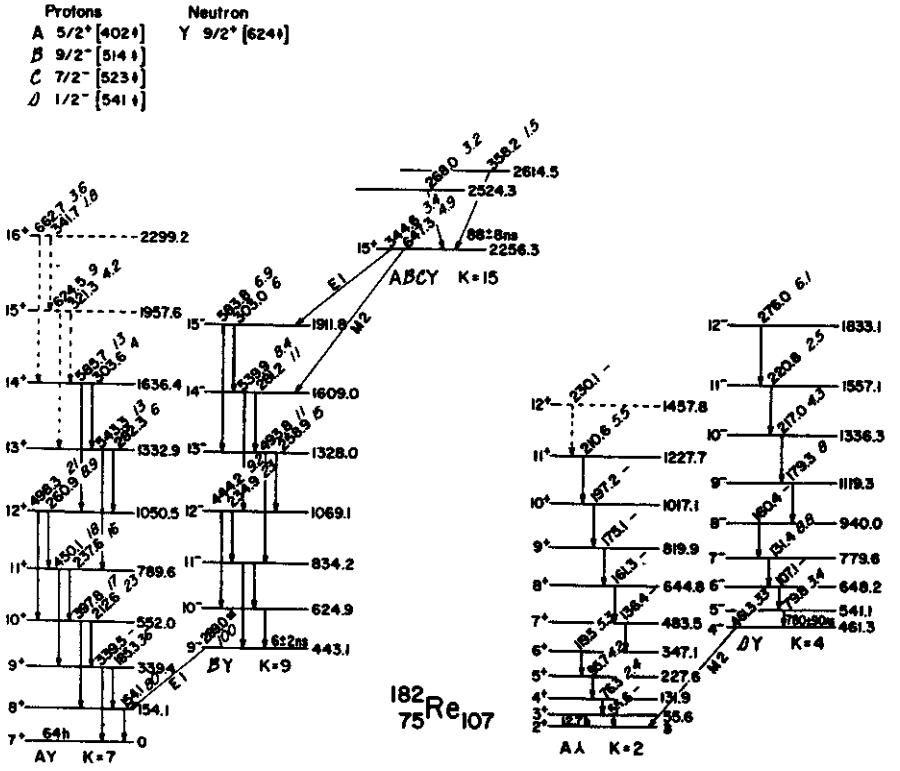

Figure 1.

negative A-term (effectively increasing the moment of inertia, so that $\hbar^2/2$ appears smaller than normal) and a positive B-term. If we examine the single-particle states involved in these bands, we find that the neutron state for all of them is the $9/2^+[624]$ Nilsson state, which originates from the $i_{13/2}$ spherical state and has very large Coriolis matrix elements; also, three of the four proton states originate from the $h_{11/2}$ or $h_{9/2}$ spherical states and have large Coriolis matrix elements. It is these states that decouple and align their spins with that of the rotating core to produce "backbending".[2] In other words, an efficient mechanism for carrying large amounts of angular momentum is for it to be shared between $\vec{R}$ of the core and $\vec{j}$ of the single nucleons. In even-even nuclei this requires the uncoupling of a pair, but in odd-odd nuclei it merely requires the selective population of aligned single-particle states. A whimsical illustration of this effect is given in Fig. 2. [Such states can be designated "klokast" (cleverest) states, in the "yrast" spirit of misusing Swedish words.] Once such states are populated in the highly-excited nucleus, normal γ-ray selection rules tend to keep the deexcitation locked into related states, the result being that only a small subset of the possible states are seen. This mechanism means that a great deal of angular momentum is tied up in the single-particle modes. For example, in the ^{182}Re level scheme the largest value of $\vec{R}$ is only 10 (in the K = 2 band), not enough to produce any drastic shifts in the moments of inertia. It will require much heavier beams to bring in larger amounts of angular momentum before phenomena such as backbending can be studied in odd-odd systems.

Odd-odd nuclei also have a head start on multi-particle states. An example of this can be seen in the 15^+ state at 2256.3 keV in ^{182}Re. A stylized illustration of this is shown in Fig. 3, where the four particles form a sort of oblate girdle about the prolate core.

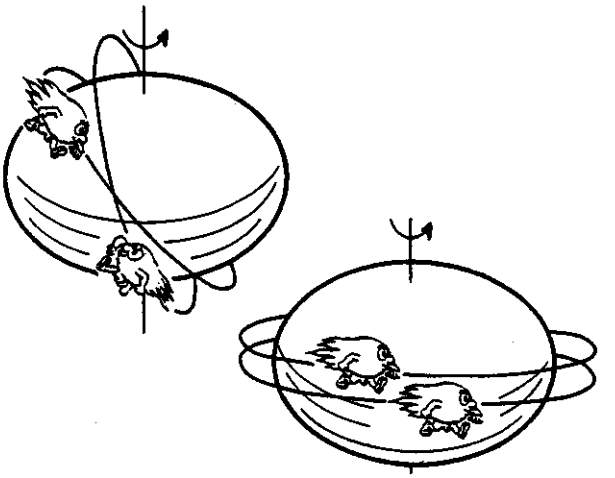

Figure 2.

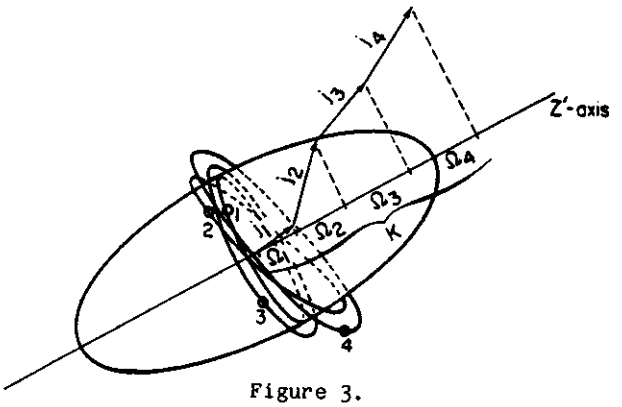

Figure 3.

Classically, an oblate spheroid rotating about its symmetry axis (oblate-||) has the largest moment of inertia and consequently produces the lowest-lying rotational states, i.e., is the most efficient in handling high angular momentum. Quantum mechanically, such rotations are not defined, of course, but it should be possible[3] to produce pseudo-rotational oblate-|| bands by having each successive "member" result from a different coupling or combination of single particles. The 15^+ state in ^{182}Re could be the beginning of such a band.

Because so much angular momentum is tied up in single-particle motion, heavier beams are needed to extend the studies. ^{182}Re is difficult to produce by heavier beams, but the lighter Re nuclei can easily be produced by

beams such as ^{14}N on Er targets. Preliminary results[4,5] for ^{180}Re and ^{178}Re show that most of the deexcitation occurs through a select few bands, which are composed of highly-aligned odd-odd states.

Although odd-odd rotational bands are best understood in well-deformed nuclei, for quite some time they have also been known to exist, based on excited states, in nuclei very close to closed shells.[6] Rather intriguing examples of this occur in many of the odd-odd Sb isotopes. The high-spin level scheme of ^{116}Sb, resulting from the $^{115}In(\alpha,3n\gamma)$ reaction,[7] is shown in Fig. 4. It contains at least two rotational bands, the J = 7 bands based on states at 1001 and 1193 keV. The former can be characterized as a relatively straightforward strongly-coupled rotational band, with the proton in the $9/2^+[404]$ orbital (originating from the $g_{9/2}$ spherical state) and the neutron in the $5/2^+[402]$ orbital (from $d_{5/2}$). The proton state again is associated with large Coriolis matrix elements. The second band is a bit more complicated, but it can be explained in a fashion silimar to that by which bands were explained[8] in ^{198}Tl. The proton can be taken basically as being in the $g_{9/2}$ orbital, which is deformation aligned (but split into the proper deformed states), while an $h_{11/2}$ neutron splits away from the core to become rotationally aligned. Calculations reproduce the observed spacings remarkably well, even down to the squashed appearance of the first several members of the band. That these rotational bands figure prominently in the deexcitation pattern is again consistent with our proposed mechanism of populating "klokast" states. Less can be said about the most prominent high-spin deexcitation pattern (at the left side of Fig. 4), for there are too many possible constructs. However, oblate-|| pseudo-rotation and rotationally aligned particles could certainly play major roles. And the other odd-odd Sb show remarkably parallel behavior.

These few examples suggest that Coriolis coupling and rotational alignment play an important part in high-spin structures of odd-odd nuclei. This can be true for nuclei near closed shells, as well as for nuclei in well-deformed regions. Selectivity caused by their operation actually simplifies rather than complicates spectra obtained in in-beam γ-ray spectroscopy. This, coupled with the abundance of relatively low-lying multi-particle states make odd-odd nuclei a fertile field for continued study.

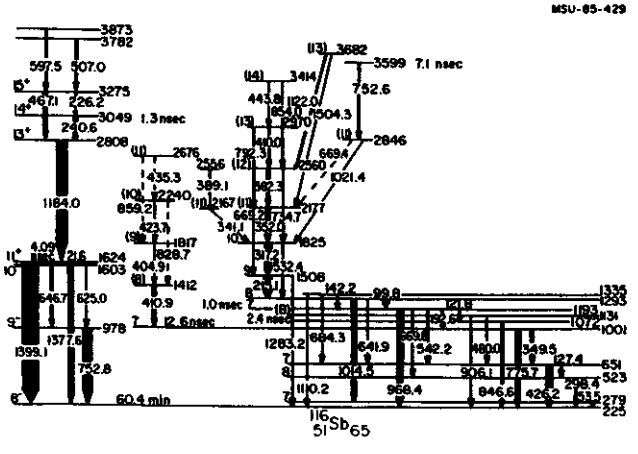

Figure 4.

References

1. M.F. Slaughter, R.A. Warner, T.L. Khoo, W.H. Kelly, and Wm.C. McHarris, Phys.Rev. C 29, 114 (1984).
2. F.S. Stephens and R. Simon, Nucl. Phys. A183, 257 (1972).
3. A. Bohr and B.R. Mottelson, Nuclear Structure (Benjamin, Reading, Mass., 1975), Vol. II, pp. 43ff, 72ff.
4. R.M. Lieder, XXIII Winter Meeting on Nuclear Physics, Bormio, Italy -- Proceedings, p. 276 (1985).
5. W.A. Olivier, W.-T. Chous, J. Kupstas-Guido, and Wm.C. McHarris, invited paper presented at the Symposium on Modern Techniques for the Study of Nuclei Off the Line of

Stability, American Chemical Society, Chicago Meeting, 12 Sept 1985; to be published in the Proceedings.
6. L.E. Samuelson, W.H. Bentley, W.H. Kelly, R.A. Warner, F.M. Bernthal, and Wm.C. McHarris, Phys. Rev. C 15, 821 (1977).
7. W.H. Bentley, R.A. Warner, Wm.C. McHarris, and W.H. Kelly, accepted for publication in Phys. Rev. C (1986).
8. H. Toki, H.L. Yadev, and A. Faessler, Phys. Lett. 71B, 1 (1977).

PARTICLE RESPONSE FUNCTION IN THE SM ISOTOPES

J.E. Duffy, G.M. Crawley, J. van der Plicht, R.S. Tickle,[a] S. Gales,[b] E. Gerlic,[c] C.P. Massolo,[c] and J.E. Finck[d]

The information obtained from the extensive[1] measurements of deep-lying hole states in nuclei is useful both for comparison with theoretical calculations and because the empirical values of position and width of particular hole states can be used as input for predictions of other nuclear phenomena such as giant resonances. However, until recently there has been little or no comparable information on highly excited particle states in medium and heavy nuclei. Measurements of the particle strength provide valuable information which is complementary to the hole strength already determined. Theoretical models have already been developed to explain the spreading of single particle strength by the mixing with both low-lying and high-lying phonon states[2-4]. While it is possible to obtain information on hole states from knockout reactions like (p,2p), there are no analogous reactions to populate particle states. Such states must be studied by transfer reactions of the kind discussed here. Understanding the potential of these reactions to provide information on high-lying particle states is therefore an additional important motivation of this work.

Some studies of particle states have recently been carried out at Orsay.[5,6] The present work is an extension to deformed nuclei. Since the spreading of the states is predicted to depend on the phonon structure, studies of deformed nuclei, in which the phonon structure is quite different from that in spherical nuclei, provide a useful test of the theory. We elected to use the even-even samarium isotopes as targets because they range from spherical to very deformed. The measurments were carried out with a 100 MeV α - beam from the K500 cyclotron, and both proton and neutron states were measured using the (α,t) and (α,^{3}He) reactions. The outgoing tritons and ^{3}He were detected cleanly in the focal plane of the S320 spectrograph.

Distinct differences are observed in the (α,t) and (α,^{3}He) spectra as the targets increase in mass and hence deformation (see Fig. 1). In these spectra we see the usual low-lying states and, at higher excitation, above 3 MeV one observes additional bound state peaks both in the (α,t) and (α,^{3}He) spectra. In the 8-16 MeV region of excitation energy, in the (α,t)

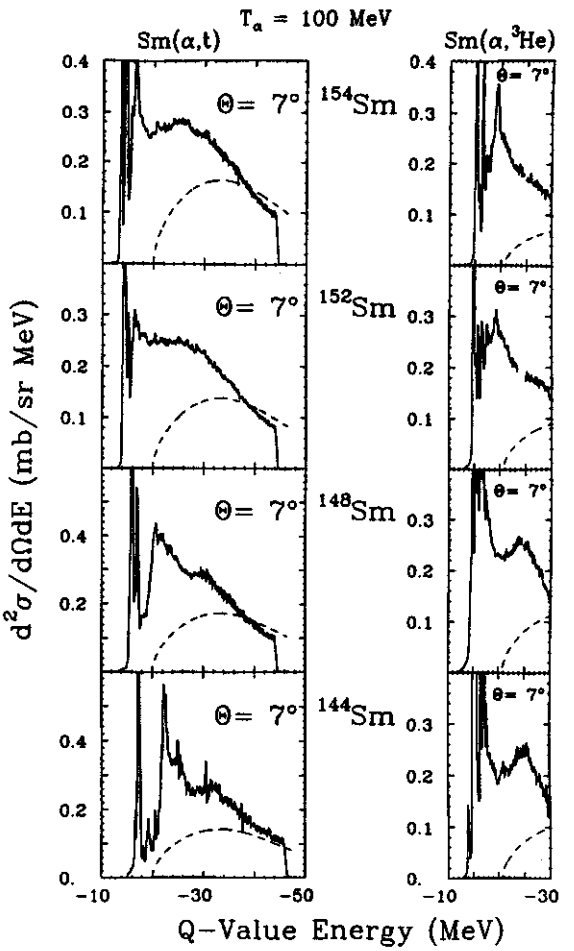

Figure 1. Spectra of tritons(left) and ^{3}He(right) scattered from ^{144,148,152,154}Sm.

spectra, we observe the development of a broad bump with increasing deformation. We observe this same phenomenon, in the (α,^{3}He) spectra, with decreasing deformation.

Not all of the cross section at high excitation energy comes from single nucleon transfer. Some of the cross section comes from elastic break up. An elastic α break up calculation[7] is shown for the ^{154}Sm (α,t) case in Fig. 2. The calculation is normalized at one

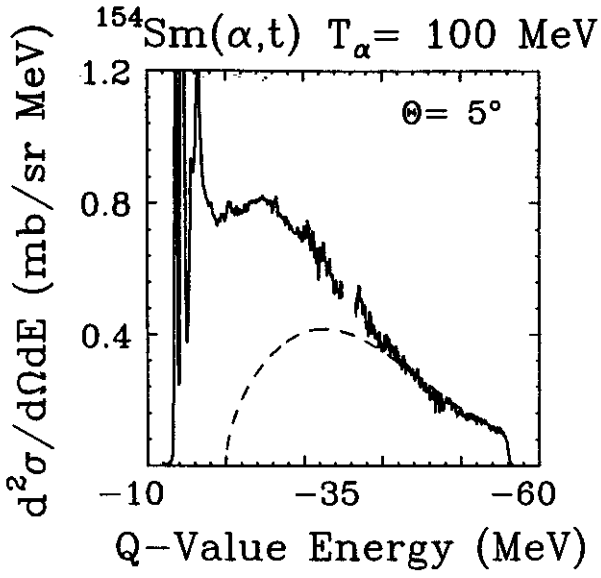

Figure 2. Spectra of tritons scattered from ^{154}Sm with the α-elastic break-up calculation.

data point, at about 30 MeV excitation for ^{154}Sm(α,t) at 5 degrees. The same normalization is used for all of the (α,t) spectra except the ^{144}Sm(α,t) spectra which requires a 6% increase in the normalization. We do not observe much cross section at about 28 MeV excitation energy in the (α,^{3}He) cases, therefore a similar background calculation does not yield a significant contribution for these spectra. This background contribution is subtracted from the spectra before further analysis of the data.

We have also tried to minimize arbitrary assumptions in determining the shape of the single-particle strength distribution. Therefore we "slice" the spectra into 520 keV bins and extract the angular distribution of the cross section for each bin. A program was developed to find the best fit of a set of DWBA calculation for different l-transfers to the extracted angular distributions for each region. From the coefficient of each DWBA l-transfer using a χ^2 minimization procedure needed for the best fit, the distributions of single-particle strength as a function of excitation energy were obtained and can be compared with theoretical predictions. We found that the minimization process picked out the known l-transfers for the low lying states (see Figure 3). This gave us

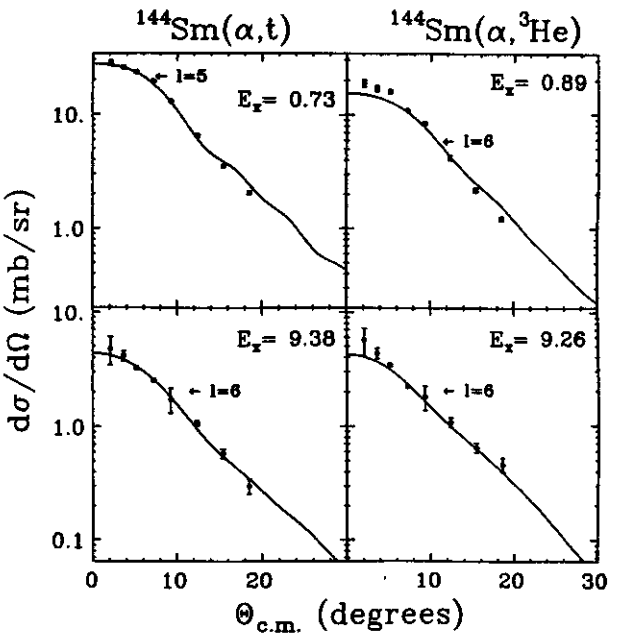

Figure 3. Angular distributions at various excitation energies of ^{144}Sm[(α,t) and (α,^{3}He)] with the fitted DWBA calculations superimposed

some confidence in the l-transfers selected for the higher excitation energies. To illustrate the minimization process, angular distributions of some low and high lying states of ^{144}Sm[(α,t) and (α,^{3}He)] are displayed in Figure 3. In this case, at the higher excitation energy, the minimization process did not pick out just one

l-transfer but a mixture of two l-transfers. However at the higher excitation energies the DWBA calulations for l=5 and l=6 are very similar in shape which makes it difficult to distinquish between the two different l-transfers. We believe that this method of extracting a strength distribution of these states is accurate to within ± 1 of the l-value stated.

Preliminary single particle strength of the states shown in Figure 3 are given in Table I.

Table I. A preliminary list of C^2S values from $^{144}Sm[(\alpha,t)$ and $(\alpha,^3He)]$ given in Figure 3.

Ex(MeV)	C^2S	l	Reaction
0.73	0.70 (±0.05)	5	$^{144}Sm(\alpha,t)$
0.89	0.23 (±0.02)	6	$^{144}Sm(\alpha,^3He)$
9.38	0.06 (±0.004)	6	$^{144}Sm(\alpha,t)$
9.26	0.09 (±0.01)	6	$^{144}Sm(\alpha,^3He)$

We observe that all of the l=5 ($h_{11/2}$) strength lies in the low lying particle states of ^{144}Sm and the l-transfers of 2, 3, 5 and 6 states are found to be fragmented over the rest of the excitation energy region. At present, the data on the Samarium isotopes is still preliminary but is presently being prepared for publication. Future work in this area will depend on how accurately the single particle strength functions can be determined by this technique. If accurate information can be obtained, further measurements will be made to allow comparison with the hole state work and with theory over a wider range of nuclei.

---

a. University of Michigan.
b. IPN, Orsay
c. IPN, Orsay and University of La Plata.
d. Central Michigan University.

References

1. G.M. Crawley. Proc. Int. Conf. on Structure of Medium-Heavy Nuclei, Osaka, Japan p590 (1980).
   S. Gales. Nuclear Physics A354,193c(1981)
2. V.G. Soloviev et al. Nuclear Physics A342,261(1980)
3. G. Bertsch et al. Physics Letters 80B,167(1969) and Rev. Mod. Phys. 55,287(1983)
4. O. Scholten, private communication
5. S. Gales et al. Phys. Rev. C 31,94(1985)
6. S. Gales, Int. School of Nuclear Structure, Alushta,USSR Oct 1985, IPN Report IPNO-DRE/85-31.
7. J.R. Wu et al. Phys. Rev. C 20,1284(1979)

THE $^{12}C(^{7}Li,t)^{16}O$ α-TRANSFER REACTION AT 80 MeV

F.D. Becchetti,[a] J. Janecke,[a] P. Lister,[a] A. Nadasen,[b] and J.S. Winfield

A high-resolution study of the $^{12}C(^{7}Li,t)^{16}O$ reaction at a laboratory energy of 80 MeV is in progress. The experiments are being carried out with the S-320 spectrometer and focal plane detector, which provide good particle identification and sufficient energy resolution to separate the low-lying states of interest.

Figure 1 shows a spectrum at 12° (lab.). The 7.12/6.92 MeV, $1^{-}/2^{+}$ doublet and the broad 9.6 MeV 1^{-} state are well resolved. The 1^{-} states are of astrophysical interest in estimations of the abundances of elements in the interstellar medium produced by helium burning (see, e.g. Ref. 1). The ratio of the yields of the 9.6 MeV to the 7.12 MeV 1^{-} states averaged over all data taken so far is about 5:1. This indicates that the 9.6 MeV state has a significantly large α reduced width and hence is expected to yield a large nucleosythesis rate of ^{16}O from the $^{12}C(\alpha,\gamma)$ reaction.

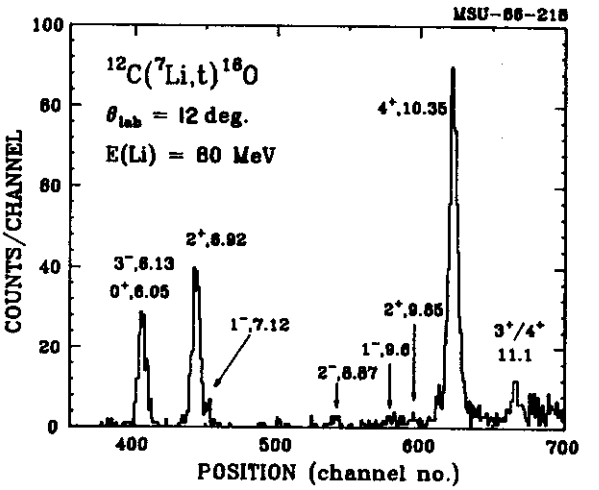

Fig. 1. A triton spectrum obtained at 12° (lab.). The spin, parity and excitation energy (MeV) of known low-lying levels in ^{16}O are indicated .

a. University of Michigan, Ann Arbor
b. University of Michigan, Dearborn

References

1. F.D. Becchetti, E.R. Flynn, D.L. Hanson and J.W. Sunier, Nucl. Phys. A305, 293(1978).

BETA LIFETIME MEASUREMENTS USING THE MSU REACTION PRODUCT MASS SEPARATOR

J. Stevenson, J.A. Nolen Jr, D. Mikolas, W. Benenson, L.H. Harwood, E. Kashy, B. Sherrill, Z.Q. Xie, and J.S. Winfield

We report results from the first experiments to use the MSU Reaction Product Mass Separator (RPMS) to study the decay properties of exotic nuclei.

In the first experiment to use the RPMS, beta-decay halflives were measured for eight neutron rich isotopes produced by fragmentation of E/A=30 MeV ^{18}O ions. The first measurements of the half-lives of ^{14}Be(4.2±0.7 ms.) and ^{17}C(202±17. ms.) have been made along with the half-lives of ^{9}Li, ^{11}Li, ^{12}Be, ^{14}B, and ^{15}B. The lifetime of ^{14}Be is one of the shortest known beta lifetimes.

The MSU RPMS is designed to separate exotic nuclei produced in intermediate energy heavy ion collisions. The RPMS separates fragments of different m/q at the focal plane making it possible to study neutron rich isotopes with m/q=3 without contamination from the more stable m/q=2 nuclei which are 10^4 times more abundant. By eliminating interfering m/q species with defining slits and concentrating the isotopes under investigation into small detectors the RPMS provides a clean environment for decay studies.

Using a 30 MeV/A ^{18}O beam, we made the first measurements of the lifetimes of ^{14}Be and ^{17}C along with the half-lives of ^{9}Li, ^{11}Li, ^{12}Be, ^{12}B, and ^{15}B during a single 48 hour run. Beta lifetimes were obtained by measuring the time interval between detection of a heavy ion and its subsequent beta decay. Beryllium and tantalum targets were used with thicknesses chosen to stop the 30 MeV/A ^{18}O beam but allow lower charge neutron rich fragments to exit the target and pass into the RPMS. The tantalum target was found to give better yields of neutron rich isotopes and was used for the measurements.

The focal plane detector consisted of a two dimensional position sensitive proportional counter followed by a silicon ΔE-E telescope using a 300 mm^2x 100 μm. (Si)ΔE and 500mm^2x5mm. (Si-Li)E detectors. Lifetime measurements were performed by turning the beam off whenever an ion with Z≥3 was detected in the telescope. The beam was left off for a preset time equal to several halflives of the longest lived isotope being collected; all beta decays in the interval were recorded. The beam is turned off in about 40 μs. by changing the phase of the rf on one of the dees of the K500 cyclotron. Isotope identification was accomplished by plotting (Fig.1) the deflection in the RPMS (proportional

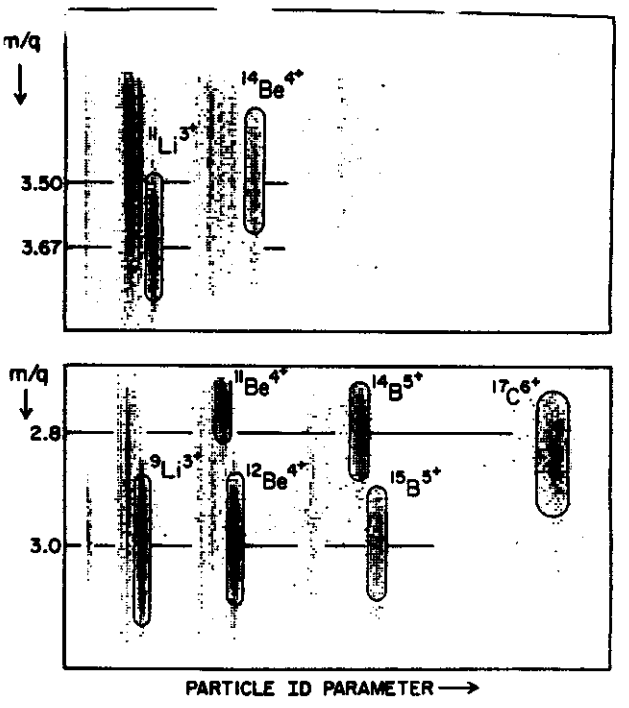

Fig. 1 Plot of m/q determined from the deflection in the RPMS vs silicon detector particle identification parameter.

to m/q) vs the silicon telescope particle identification function. The decay curves are shown in figure 2. The curves are best fits to an exponential plus a constant background.

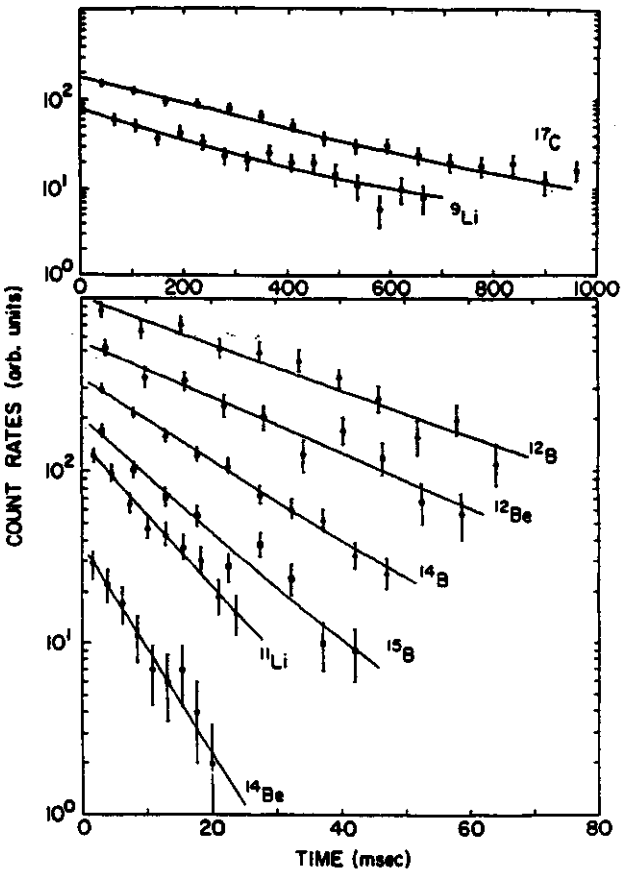

Fig. 2 Beta lifetime plots, the curves are best fits to an exponential plus constant background form.

The analysis of ^{14}Be and ^{12}Be is complicated by the daughter nucleus being rather shortlived. For these two isotopes, events were required to have a second beta within two daughter half-lives in order to be included in the lifetime spectrum.

The results of this experiment are compared with previous measurements in table I.

Table 1:

Isotope	This Measurement	Previous Measurement	Prediction[f]
^{9}Li	173±14 ms	175±1 ms[a]	76 ms
^{11}Li	7.7±0.6 ms	8.5±0.2 ms[a]	2.3 ms
^{12}Be	21.3±2.2 ms	24.4±3.0 ms[b]	8.8 ms
^{14}Be	4.2±0.7 ms	----	3.7 ms
^{12}B	20.0±1.5 ms	0.41±0.6 ms[c]	13.6 ms
^{14}B	12.8±0.8 ms	16.1±1.2 ms[d]	11.1 ms
^{15}B	8.8±0.6 ms	11.0±1.0 ms[e]	6.2 ms
^{17}C	202±17 ms	---	(414,292,238)ms

Beta decay half-lives for the neutron-rich isotopes measured in this experiment are compared with previous measurements when they exist. Theoretical predictions for Gamow-Teller beta decay are also provided for comparison. The three theoretical halflives for ^{17}C correspond to the asumption of ($1/2^+$, $3/2^+$, $5/2^+$) ground state J^π values for ^{17}C in the calculation.

a) Ref 6
b) Ref 4
c) Ref 3
d) Ref 1
e) Ref 5
f) Ref 2

There are two cases of discrepancies outside of one standard deviation, ^{14}B and ^{15}B. In both cases there was only one previous measurement, and there is no obvious reason for the discrepancies. It is possible that the background under the ^{14}B decay curve of ref. 1 was underestimated leading to the larger value of the extracted lifetime.

For the nuclei studied in this experiment the dominant decay mode is Gamow-Teller beta decay. Partial halflives corresponding to Gamow-Teller beta decay calculated in a spherical shell model formalism[2] are shown in table I. The calculated lifetimes are with one exception(^{17}C) shorter than the measured lifetimes.

In conclusion the first half-life measurements of light neutron rich nuclei using the MSU Reaction Product Mass Separator have resulted in the measurement of eight halflives, two of which represent first time measurements and three of which are second measurements. The RPMS coupled with fast beam switching provides a very clean environment in which to study the decays of neutron rich nuclei.

References

1. D. E. Alberger and D. R. Goosman, Phys. Rev. C10, 912 (1974).
2. B. A. Brown private communication
3. F. Ajzenberg-Selove, Nucl. Phys. A248, 1 (1975).
4. D. E. Alberger, et. al., Phys. Rev. C17, 1525(1978).
5. J. P. Dufour, et. al. Preprint CENBG 8430.
6. E. Roeckl, P.F. Dittner, C. Detraz, R. Klapisch, C. Thibault, And C. Rigaud, Phys. Rev. C10, 1181 (1974).

BETA DECAY BRANCHING RATIOS OF ^{9}C

J. Stevenson, J.A. Nolen Jr, D. Mikolas, W. Benenson, L.H. Harwood, E. Kashy, R. Sherr*, B. Sherrill, Z.Q. Xie, and J.S. Winfield

Several experiments[1] comparing the beta decay branching ratios of mirror nuclei have found significant departures from mirror symmetry. These departures have been attributed[2] to an induced tensor term in beta decay. This would cause the largest departures from mirror symmetry for light mirror pairs. One of the lightest mirror pairs ^{9}Li and ^{9}C has not been studied due to the lack of data on ^{9}C branching ratios. The difficulty with studying ^{9}C beta decay is that the excited states in the daughter ^{9}B do not decay by gamma emission but by $^{9}B \rightarrow {}^{4}He + {}^{4}He + p$.

Beta decay branching ratios of ^{9}C were measured by implantation of E/A=15 MeV ^{9}C ions in a silicon detector telescope. The ^{9}C ions were produced by bombardment of a Ni target with a beam of E/A=35 MeV ^{12}C ions. The ^{9}C ions were collected with the NSCL Reaction Product Mass Separator.

When a ^{9}C ion was detected in the silicon detector telescope the cyclotron was turned off for .5 seconds(in 40 μS), and the silicon detector preamplifier gain was increased by a factor of 10. The beta decay of ^{9}C to various states in ^{9}B is followed by the prompt(10^{-18} sec) decay of ^{9}B by $^{9}B \rightarrow {}^{4}He + {}^{4}He + p$. The low energy decay products of ^{9}B are completely contained in the silicon detector but the beta energy loss is rather small(~300 KeV). Thus the decay energy observed in the silicon detector is primarily due to the excitation energy of the state in ^{9}B and thus determines the state in ^{9}B to which the ^{9}C decayed.

Figure 1 shows the decay energy energy spectrum of ^{9}C.There are two distinct peaks which appear in the spectrum. The lowest energy peak at about 600 KeV corresponds to decays to the ground state in ^{9}B. The known decay energy

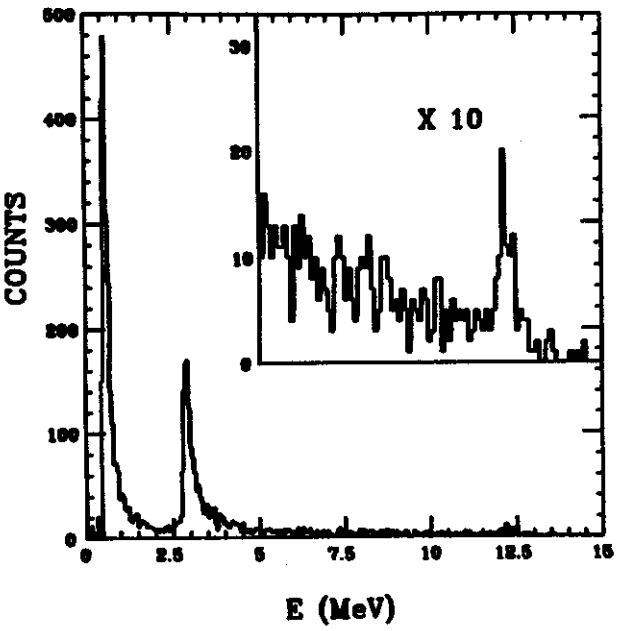

Fig. 1 Measured ^{9}C decay energy spectrum. The insert shows the spectrum above 5 MeV on an expanded scale.

of the ^{9}B ground state is 277 KeV. Thus roughly half the energy observed(or 300 KeV) is due to beta energy loss in the silicon. The second major peak is at about 2.7 MeV and is due to decay to the known $5/2^{-}$ state in ^{9}B at 2.36 MeV[3]. Less striking features include a small peak at about 12.3 MeV. The are two nearby reported states in ^{9}B 11.7 MeV and 12.06 MeV. The reported widths on the states are both about 800 KeV which is considerably wider than the 400 KeV width we observe. Additional features are a broad peak near the $5/2^{-}$ state which is believed to correspond to a recently observed $1/2^{-}$ state at 2.6 MeV with an observed width of 1.6 MeV. Finally there is a significant branch to unresolved states between 4 and 11 MeV.

Table 1 contains the measured branching ratios for ^{9}C beta decay and compares them to

Table 1

^{9}Li Decay		^{9}C Decay	
State in ^{9}Be	% Branch	State in ^{9}B	% Branch
g.s. $3/2^-$	50.5±5.	g.s. $3/2^-$	43.±5.
2.43 $5/2^-$	34.±4.	2.36 $5/2^-$	22.±5.
2.8 $1/2^-$	10.±2.	2.6 $1/2^-$	16±5.
7.94 $(1/2)^-$	1.5±.5	5 to 12	17.8±5.
11.28 $(3/2)^-$	4-X.5	11.7	1.2±.3

Table 1: Comparison of ^{9}Li and ^{9}C beta branching ratios.

previously measured[3] branchiong ratios for the decay of the mirror nucleus ^{9}Li. The branching ratios of the mirror decays are in qualitative agreement.

References

1. J. E. Esterl, J. C. Hardy, R. G. Sextro, and J. Cerny Physics Letters 33B 287, (1970).
2. D. H. Wilkinson Physics Letters 31B 447,(1970).
3. M. Langevin, C. Detraz, D. Guillemaud, F. Naulin, M. Epherre, R. Klapisch, S. K. T. Mark, M. De Saint Simon, C. Thibault, F. Touchard Nuclear Physics A366 449,(1981). 1 (1975).

ELASTIC AND INELASTIC SCATTERING OF 35 MEV/A ^{6}LI IONS FROM ^{12}C, ^{58}NI ^{90}ZR AND ^{208}PB

M. McMaster,[a] G. Gunderson,[a] A. Judd,[a] S. Villanueva,[a] A. Nadasen,[a] F. D. Becchetti,[b] J. Janecke,[b] P. Schwandt,[c] J. Winfield, J. van der Plicht, R.E. Warner,[d] and A.A. Cowley[e]

We have made measurements of the elastic scattering of 35 MeV/A ^{6}Li ions over wide center-of-mass angular ranges using the S320 spectrometer. Differential cross section data were obtained for ^{12}C(3°-61°), ^{58}Ni(3°-48°), ^{90}Zr(3°-44°), and ^{208}Pb(3°-36°). The relative errors are generally of the order of 3%, except for the largest angles where they are ~10%.

The data for ^{12}C are shown in Fig. 1 (circles) where it can be observed that the cross sections span seven orders of magnitude. Diffractive oscillations extend up to ~30°, followed by exponential fall-off characteristic of rainbow scattering. The onset of rainbow scattering for ^{58}Ni (Fig. 2) occurs at ~33°. For ^{90}Zr it is about 35°. The data do not reach the rainbow region for the ^{208}Pb target.

These data provide important advances in our understanding of the ^{6}Li-nucleus interaction. From the macroscopic point of view, a realistic analysis in terms of the phenomenological optical potential can be made. Data at lower energies have not been able to resolve the discrete ambiguities in the potentials because of lack of measurements beyond the rainbow angle. The present data seem to provide unique potentials. The calculations for ^{12}C are shown as the solid curve in Fig. 1. The parameters are listed in Table I. The derived volume integral is in excellent agreement with other light-ion unique potentials.[1] Preliminary analysis of the ^{58}Ni data indicate similar agreement. The global analysis of all the data is in progress. The general applicability of potential-folding models to the scattering of composite projectiles has provided the principal motivation for the present experiment with ^{6}Li ions. Although the calculation of complex-

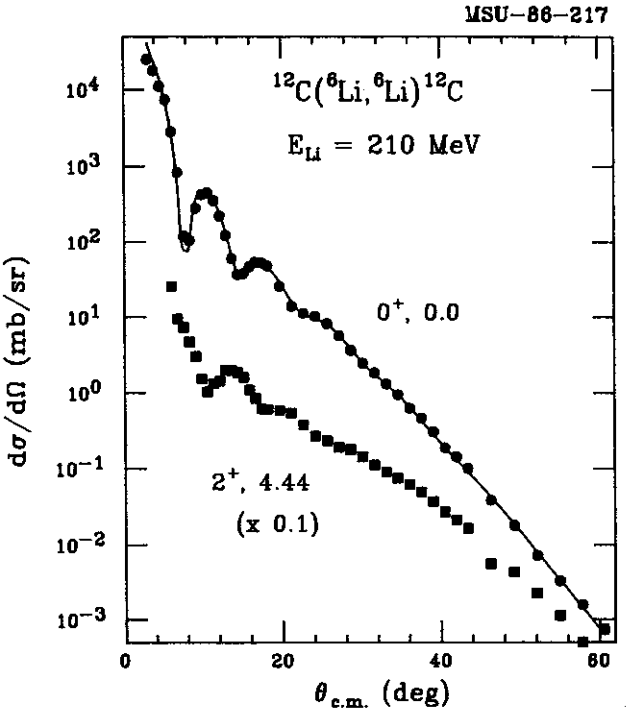

Fig. 1 Angular distributions for the elastic scattering (circles) and inelastic scattering (squares) of ^{6}Li on ^{12}C at 210 MeV. The solid lines represent optical model fits to the data.

Table 1: Optical model parameters deduced for ^{6}Li + ^{12}C at E(^{6}Li)=210 MeV.

V	r_o	a_o	W_V	r_w	a_w	r_c	$J_R/6A$
121.7	1.206	0.818	37.72	1.546	0.865	1.2	279.

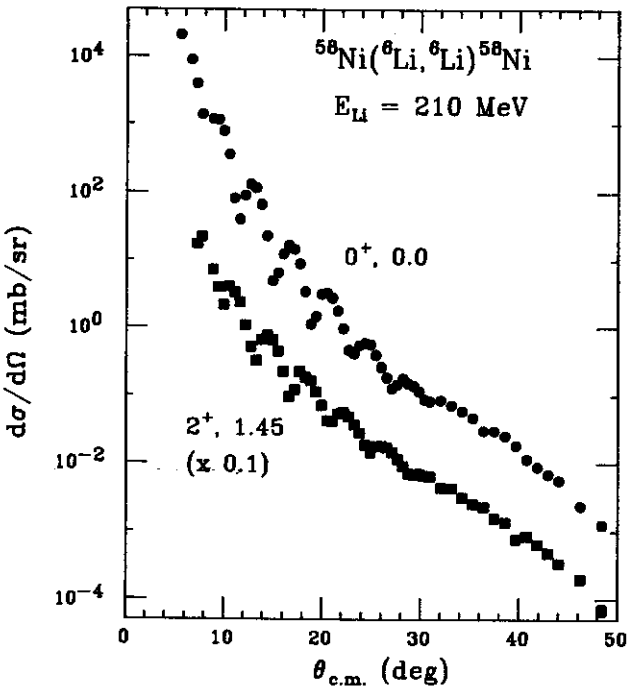

Fig. 2 Angular distributions for the elastic scattering (circles) and inelastic scattering (squares) of ^{6}Li on ^{58}Ni at 210 MeV.

projectile optical potentials using the single-nucleon optical potential and a detailed model for the structure of the projectile can generally be expected to become more difficult as the number of nucleons in the projectile increases, a simplification arises for the ^{6}Li projectile as a result of its well-developed cluster structure, namely, a weakly bound α+d system. Thus the ^{6}Li optical potential is calculated[2] to lowest order simply by convolution of a well-understood α-n optical potential with the α+d cluster model wave function for ^{6}Li as an alternative to the N-n and ^{6}Li-N folding models.

Both a single-folding ^{6}Li potential based on an (α+d)-cluster model for ^{6}Li (Ref. 3) and double-folding potentials generated from a realistic nucleon-nucleon interaction[4] have provided a reasonable description of the low energy data. However, the calculated real potentials required a renormalization of 0.5 to 0.7 in order to fit the data. These calculations neglect the distortion and breakup of the ^{6}Li in the field of the nucleus. Another factor to be considered is the Pauli exclusion principle. This would, of course, decrease the potential in the nuclear interior. It is clear that the folding model calculations for ^{6}Li elastic scattering require additional refinements. It is hoped that the present data, because of their broad angular range, will shed some light on the problems associated with the existing folding models.

Further, comparison of results for ^{6}Li with those obtained for the α-nucleus interaction[1] on the one hand and those from light heavy-ion scattering (e.g. ^{12}C, ^{16}O) on the other hand should provide a more systematic insight into the validity, limitations, and relative merits of the various folding approaches as a function of projectile mass. Specifically, these investigations for ^{6}Li, together with previous work for d and α-particles, are meant to provide information on density-dependent effects in nuclear interactions of increasingly more complex scattering systems.

Differential cross sections for the inelastic scattering of ^{6}Li ions leading to the first excited states of the target nuclei were obtained concurrently with the elastic scattering data. The inelastic scattering data for ^{12}C and ^{58}Ni are shown in Figs. 1 and 2 (squares). In all cases the inelastic cross section magnitudes are comparable to those of the elastic at large angles. In fact for ^{12}C the inelastic cross section exceeds the elastic cross section for $\theta_{cm} > 36°$. This is an indication that coupled channel calculations may be important in the analysis of the data.

---

a. University of Michigan, Dearborn
b. University of Michigan, Ann Arbor
c. Indiana University, Bloomington
d. Oberlin College, Ohio
e. CSIR, South Africa

References

1. D.A. Goldberg et al., Phys. Rev. C7, 1938 (1973); ibid C10, 1362 (1974).
2. J.W. Watson, Nucl. Phys A198, 129 (1972).
3. P. Schwandt et al., Phys. Rev. C24, 1522 (1981); ibid C21, 1656 (1980); J.Janecke, F.D. Becchetti and D. Overway, Nucl. Phys. A343, 161 (1980)
4. D.P. Stanley, F. Petrovich and P. Schwandt, Phys. Rev. C22, 1357 (1980)